

# We are IntechOpen, the world's leading publisher of Open Access books Built by scientists, for scientists

6,900

Open access books available

186,000

International authors and editors

200M

Downloads

Our authors are among the

154

Countries delivered to

TOP 1%

most cited scientists

12.2%

Contributors from top 500 universities



WEB OF SCIENCE™

Selection of our books indexed in the Book Citation Index  
in Web of Science™ Core Collection (BKCI)

Interested in publishing with us?  
Contact [book.department@intechopen.com](mailto:book.department@intechopen.com)

Numbers displayed above are based on latest data collected.  
For more information visit [www.intechopen.com](http://www.intechopen.com)



# Smart Surfaces with Tunable Wettability

*Meenaxi Sharma and Krishnacharya Khare*

## Abstract

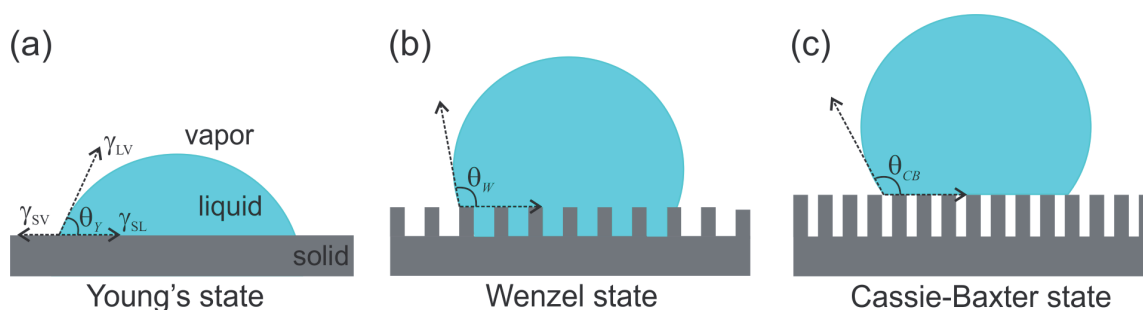
Modification of surface wettability (ranging from complete wetting to complete non-wetting) of various surfaces is often required in many applications. Conventionally, it is done using a coating of suitable materials as per the requirement. In this approach, the old coating needs to be replaced every time by a new appropriate one. Alternatively, smart responsive surfaces can show tunable wettability with external stimulus. Electric field, temperature, light, pH, mechanical strain, etc. can be effectively used as external stimuli, and a suitable coating can be incorporated, which responds to the respective stimulus. These surfaces can be used to tune the surface wettability to any extent based on the magnitude of the stimulus. The primary role of the external stimulus is to vary the liquid-solid interfacial energy, which subsequently changes the surface wettability. The biggest advantage of this approach is that the surface wettability can be reversibly tuned. Each of the techniques mentioned above has many advantages along with certain limitations, and the combination of advantages and limitations helps users to choose the right technique for their work. Many recent studies have used this approach to quantify the tuning of the surface wettability and have also demonstrated its potential in various applications.

**Keywords:** wetting, surface energy, tunable wetting, responsive surfaces

## 1. Introduction

There are numerous examples in our daily life where we encounter liquid-solid interaction, for example, wall paints, cookwares, cleaning textiles, raindrops on glass surfaces of automobiles, houses, solar panels, to name a few. In all these examples, drops of different liquids interact with given solid surfaces. The macroscopic behavior of liquids on such solid surfaces is actually governed by the microscopic molecular interactions between the liquid and solid molecules, which in scientific terms is described as the wetting behavior of solid surfaces. **Figure 1** shows the schematics of liquid drops on homogeneous and heterogeneous surfaces describing their final wetting behavior. **Figure 1a** shows Young's wetting state of a liquid drop sitting on a homogeneous surface where the surface wettability is described in terms of Young's contact angle ( $\theta_Y$ ), which can be derived by balancing various interfacial forces ( $\gamma$ 's) as given by Eq. (1) where  $S$ ,  $L$ , and  $V$  represent solid, liquid, and vapor phases respectively [1].

$$\cos\theta_Y = \frac{\gamma_{SV} - \gamma_{SL}}{\gamma_{LV}} \quad (1)$$

**Figure 1.**

Schematics of different wetting states of a liquid drop on a homogeneous surface: (a) Young's state and heterogeneous surface; (b) Wenzel and (c) Cassie-Baxter states.

On heterogeneous surfaces, as shown in **Figure 1b, c**, the final wetting behavior is different compared to homogeneous surfaces and is described by Wenzel and Cassie-Baxter contact angles as given by Eq. (2) [2, 3]:

$$\cos\theta_W = r \cos\theta_Y \quad \text{and} \quad \cos\theta_{CB} = f \cos\theta_Y + (f - 1) \quad (2)$$

where  $r$  is the roughness factor, and  $f$  is the area fraction of the solid-liquid interface.

In many cases, maximum interaction of liquid-solid is required, for example, washing textiles, wall paints etc., whereas there are other cases where minimum liquid-solid interaction is desirable, for example, solar panel, nonstick cookware, and glass windshields. Therefore, it becomes essential to manipulate liquid-solid interaction or wetting behavior as per the requirement. Alternative to the conventional approach, where the wetting behavior is manipulated by varying the surface topography or chemistry, continuously and reversibly varying the wettability based on some external energy source has recently gained huge popularity. This method has many advantages over the conventional method due to its nondestructive nature. Various researchers and engineers have investigated many such external energy sources or stimuli (e.g., electric field, temperature, radiation, mechanical strain, pH, magnetic field, etc.), which can be efficiently used to manipulate the wetting behavior of given solid surfaces continuously as well as reversibly. In this chapter, we provide a comprehensive summary of most of these techniques with the fundamental principle behind them as well as their potential applications.

## 2. Smart responsive surfaces

Based on the nature of external stimuli used to manipulate the wettability of a given surface, smart responsive surfaces can be divided into many categories, which are discussed in the following sections. Each of the smart surfaces has some advantages and disadvantages over others, which is discussed in depth along with their fundamental mechanism, state-of-the-art status, and potential commercial applications.

### 2.1 Electric field-responsive surfaces

An electric field as an external stimulus is considered to be one of the fast and convenient ways to switch the surface wettability by virtue of its ability to control the surface chemistry in a few seconds or less. This is one of the most versatile ways to manipulate the liquids on solid as well as liquid surfaces without applying a responsive coating on the surface. However, to perform the

electrowetting experiment, it is mandatory to have both the substrate and the liquid to be conducting. The electrowetting phenomenon, which is based on the electrocapillarity principle, was first explained in detail by Lippmann in 1875 [4, 5]. Traditional electrowetting was started around 1973 where the electrocapillarity technique was applied to a three-phase system in which a drop of the aqueous electrolyte solution was in contact with a mercury substrate [6]. Later in 1993, developments in this field were commenced by Berge et al. who gave the idea of introducing a thin insulating layer to avoid the direct contact between the conducting drop and the electrode in order to get rid of the electrolysis of water, which is also known as the electrowetting on dielectrics [7]. The electrowetting phenomenon is known to be the dependence of the contact angle on the applied potential between the conducting drop and the conducting substrate. In the electrowetting process, with the applied voltage, a reduction was observed in the interfacial tension of the solid-liquid interface, which further leads to decrease the observed contact angle without affecting the chemical composition of the substrate (as shown in **Figure 2A**).

$$\gamma_{SL}(V) = \gamma_{SL}(0) - \frac{\epsilon_0 \epsilon_d}{2d} V^2 \tag{3}$$

where  $\epsilon_0$  is the permittivity of vacuum,  $\epsilon_d$  is the dielectric constant of the insulating material,  $d$  is the thickness of the insulating layer, and  $V$  is the applied voltage.

Berge proposed the electrowetting equation by energy minimization method to get the relationship between the contact angle and the applied voltage, also known

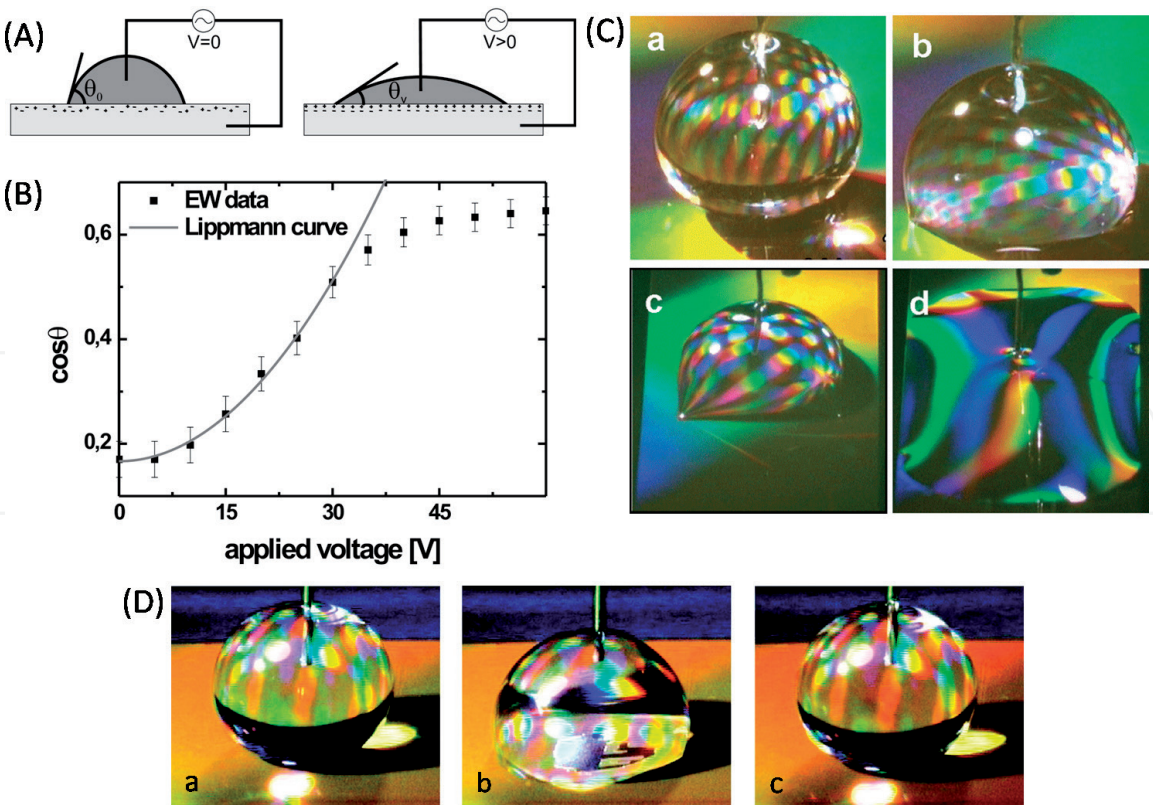


**Figure 2.**  
(A) Sketch of the electrowetting setup on a dielectric (EWOD). The droplet and the conducting Si substrate form a capacitor with the dielectric SiOx layer. (B) Electrowetting curve for the system consisting of triangular grooves used in the experiments reproduced with permission from [8]. (C) Four frames from the video recording demonstrating electrically induced transitions between different wetting states of a liquid droplet on the nanostructured substrate reproduced with permission from [9]. (D) Demonstration of electrically induced reversible transitions between different wetting states of a liquid on a nanostructured substrate, reproduced with permission from [10].



as the famous Young-Lipmann equation [7]. In the absence of trapped charges, the equation can be derived as:

$$\cos\theta(V) = \cos\theta(0) + \frac{\varepsilon_0 \varepsilon_d}{2\gamma_{LV}d} V^2 \quad (4)$$

where  $\theta(0)$  and  $\theta(V)$  represent the contact angle without applied voltage and at a finite voltage  $V$ , respectively.

However, if the trapped charges are present, a finite voltage  $V_T$  of the trapped charges should get introduced in the above equation, and the modified equation can be written as

$$\cos\theta(V) = \cos\theta(0) + \frac{\varepsilon_0 \varepsilon_d}{2\gamma_{LV}d} (V - V_T)^2 \quad (5)$$

where  $V_T$  is the voltage to consider the effect of trapped charges. According to this equation, the contact angle continuously decreases with increase in the applied voltage. However, beyond the threshold voltage, the contact angle is found to be independent of the applied voltage, and this phenomenon is called the contact angle saturation (as shown in **Figure 2B**). It is difficult to achieve a large change and reversible initial contact angle with the applied voltage. In practice, the reversible electrowetting can only be achieved for small voltage change due to contact angle saturation phenomenon at high voltages (as shown in **Figure 2B**).

Inspired by nature, surfaces with micro/nanostructures give rise to superhydrophobic behavior with a larger water contact angle. On the contrary, electrowetting reduces the initial contact angle by the applied voltage. Combining superhydrophobicity with electrowetting would lead to effectively enhance the range of wettability change. Electrowetting on micro/nanostructured surfaces has acquired a lot of attention in the research community from various aspects, from fundamentals to applications [9, 11–15]. For the first time, Krupenkin et al. demonstrated the electric field-controlled dynamic wetting behavior of liquids on nanostructured surfaces [9]. They had shown that electrowetting was a tool to dynamically control the wetting behavior of liquids by covering a wide range of wetting states from superhydrophobic (non-wetting) to almost complete wetting as shown in **Figure 2C**. When no voltage was applied, drop took the shape of a spherical ball with a contact angle close to  $180^\circ$  (**Figure 2C—(a)**). With an increase in the applied voltage to 22 V, it underwent a transition to the immobile state with a decrease in the contact angle (**Figure 2C—(b, c)**). With a further increase in the voltage to 50 V, the contact angle decreased, making a transition to the completely wetting state (**Figure 2C—(d)**). Later, they extended their work to focus on the electric field-induced reversible wetting transition between the non-wetting state (Cassie-Baxter) and the partial wetting state (Wenzel) on a nanostructured surface [10]. They have shown the controlled reversible wetting transition between a rolling drop and a completely immobile drop on a nanostructured surface. To reverse the transition from the immobile state to the rolling drop, they transported a short pulse of electric current through the nanostructured substrate. One of the major issues associated with the electrowetting experiment is the large contact angle hysteresis, that is, difference between the contact angle values after the completion of one voltage cycle, that is, after the voltage has reached to 0 V.

In the past decade, many research groups have dedicatedly worked on the minimization of contact angle hysteresis during electrowetting on smooth as well rough surfaces [16–18]. To achieve the reversible electrowetting, a lubricating fluid can be used to cover the surface structures to provide a smooth layer of lubricating fluid on top of the dry substrate to reduce the surface hysteresis to a large extent by

minimizing the undesirable energy loss [19–21]. Hao et al. performed electrowetting on liquid-infused film (EWOLF) to get complete reversible wetting behavior. They have shown that infusing the lubricating fluid in porous membranes, and viscous energy dissipation could be sufficiently enhanced with suppression of drop oscillation, resulting in fast response without losing the reversible behavior [20]. Upon applying a voltage of 500 V, the contact angle decreased to 50° on the lubricant-infused membranes showing a wettability change of 53° (**Figure 3a**).

Careful observation reveals that wetting ridges are formed at the oil-water interface due to the deformation of the lubricant caused by the capillary pressure (**Figure 3b**). Due to the presence of a smooth liquid-liquid interface, drop freely moves without any pinning and turns back to its initial wetting configuration indicating complete reversible behavior (**Figure 3c**). However, for the superhydrophobic PTFE membranes, due to large electrowetting hysteresis, the wetting transition was irreversible. Measurement of apparent contact after every voltage on-off cycle also confirms the electrowetting reversibility for liquid-infused membranes (**Figure 3d**). Electrowetting hysteresis on the liquid-infused membranes (~3°) is much smaller compared to the superhydrophobic membranes (~40°). Later Bormashenko et al. also reported the low voltage electrowetting on EWOLF utilizing lubricated honeycomb polymer surfaces with very low contact angle hysteresis [22]. Due to fast response, reversible wetting behavior, and low energy consumption, electrowetting has gained a lot of attention among various researchers for its applications in emerging fields such as liquid lens [23, 24], optical display [25], liquid patterning, and controlled movement of liquid drops in narrow channels. One of the most important applications realizing electric field-induced tunable

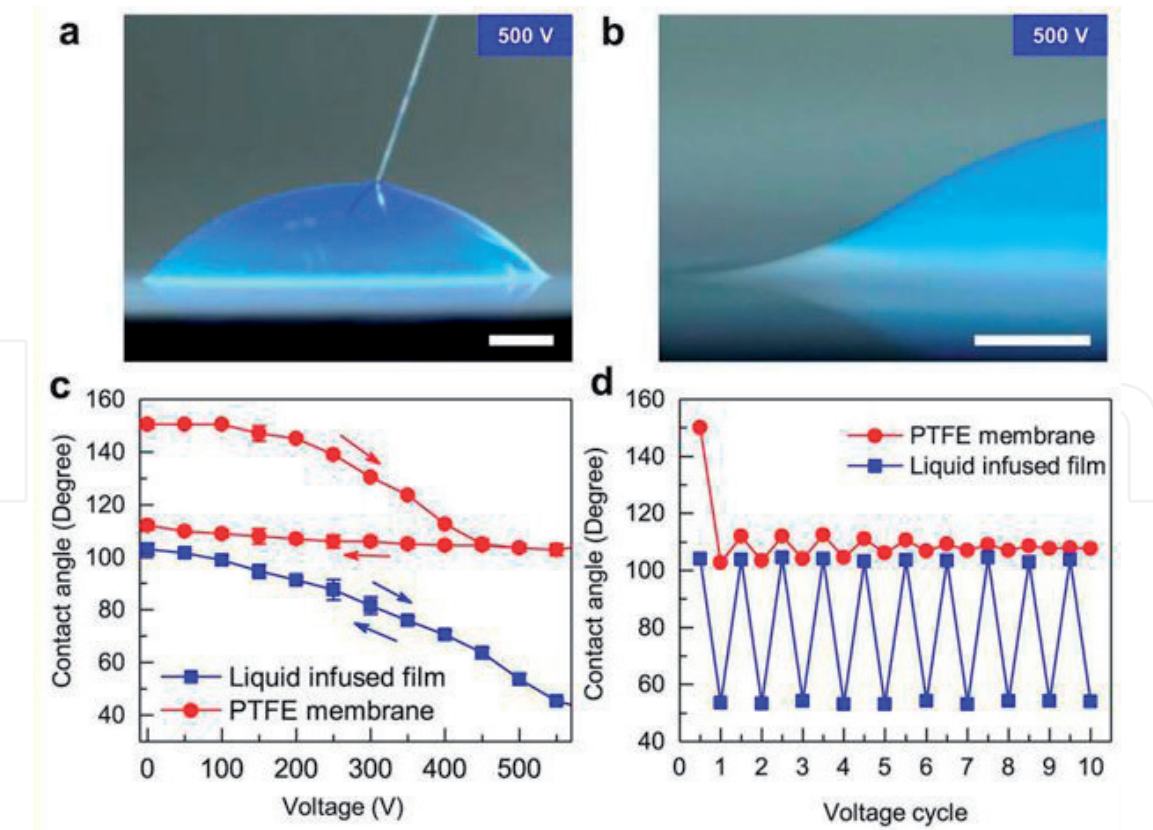
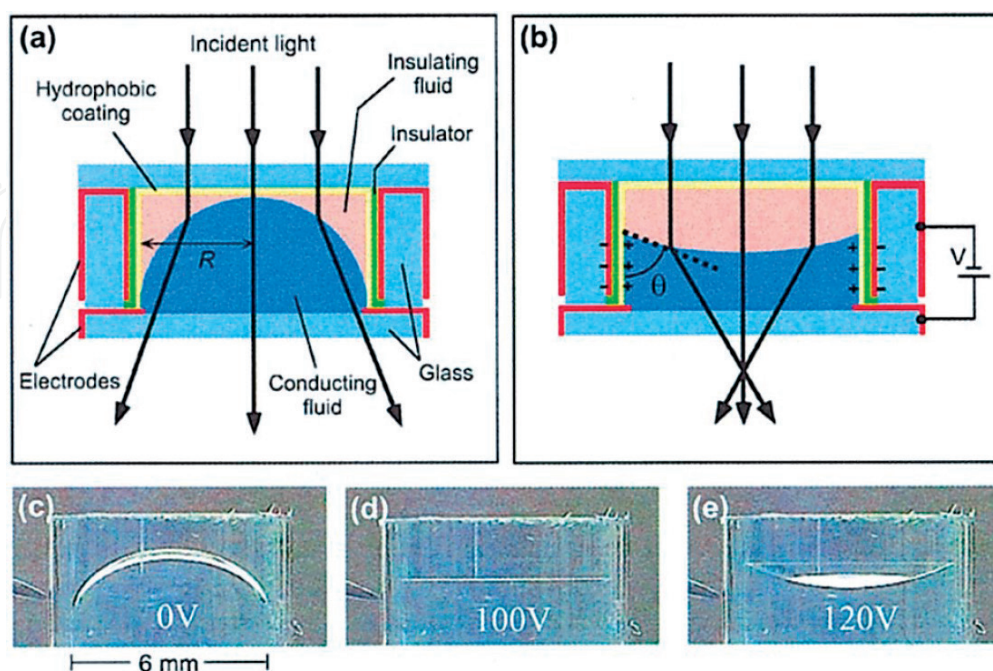


**Figure 3.** Wetting properties of liquid-infused film and electrowetting response. (a) Optical image of a stained droplet in EWOLF subject to an actuation voltage of 500 V. (b) the formation of the wetting ridge as a result of oil motion at the liquid-liquid interface. (c) Characterization of the variations of apparent CA in EWOD and EWOLF. (d) The variation of droplet apparent CA subject to electrowetting cycles. Reproduced with permission from [20].

wettability is an optical zoom lens [23, 24]. Kuiper has demonstrated a liquid-based variable focal lens based on the meniscus between two immiscible liquids. The application of voltage would result in the accumulation of charges near the solid-liquid interface, which would further lead to change the shape of the meniscus from convex to concave, as shown in **Figure 4** [24].

## 2.2 Temperature-responsive surfaces

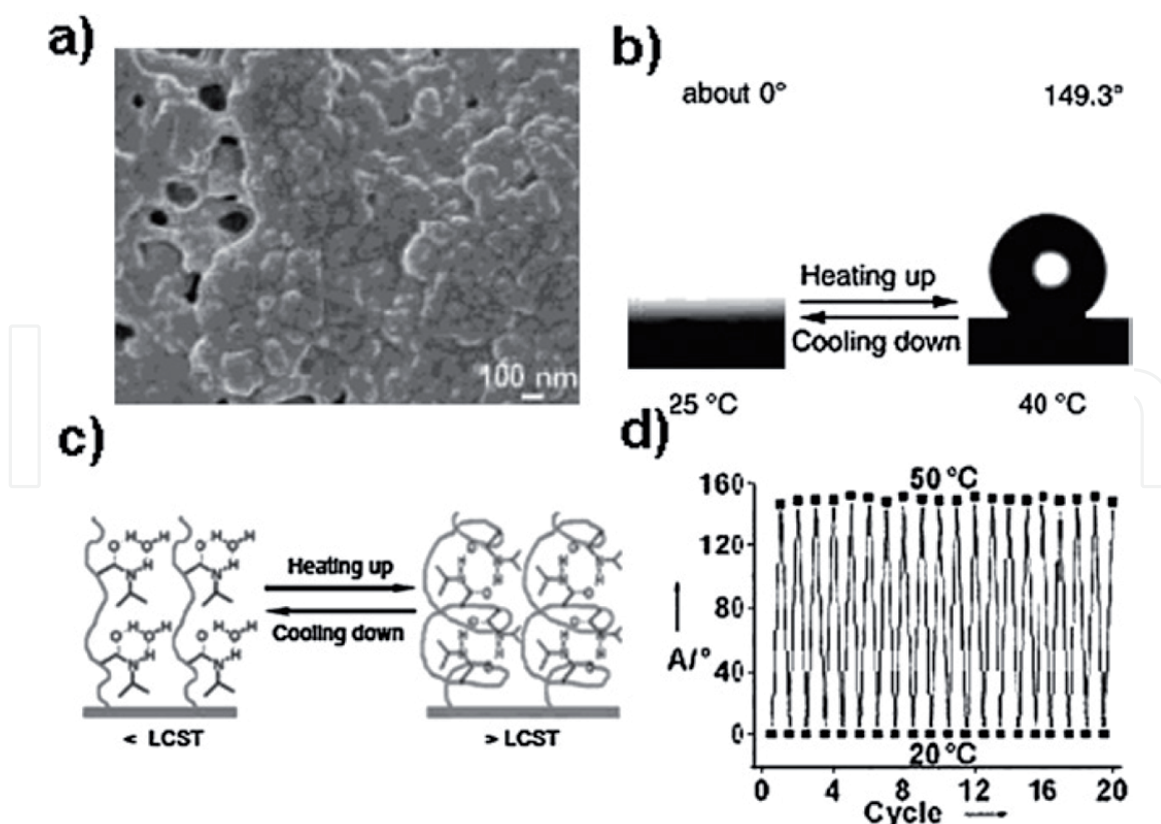
Temperature-responsive or thermoresponsive polymers often evince a conformational change of polymer chains in response to the temperature change, and they are widely used to develop thermoresponsive surfaces [26]. Polyisopropylacrylamide (PNIPAAm), the most common temperature-responsive polymer, shows different molecular arrangement at temperatures below and above the lower critical solution temperature (LCST) of about 32°. Below LCST, the intermolecular hydrogen bonding between the amino groups and carbonyl groups as well as water leads to a loosely coiled molecular arrangement resulting in hydrophilic behavior. While above LCST, the intramolecular hydrogen bonding leads to form a compact and collapsed arrangement of PNIPAAm chains, hence making it difficult for carbonyl and amino groups to interact with the water molecules and results in the hydrophobic behavior. PNIPAAm films can be easily grafted on both smooth as well as rough substrates using surface-initiated atom transfer radical polymerization (ATRP) technique. However, on smooth substrates modified with PNIPAAm coating, wettability change was limited as demonstrated by Sun et al. that wettability could only be varied from 63 to 93° by changing the temperature below and above LCST [27]. By introducing the roughness, thermoresponsive wettability of the surface was greatly enhanced, and a large reversible wettability switch from superhydrophobic ( $\sim 149.3^\circ$ ) to superhydrophilic ( $\sim 0^\circ$ ) was achieved [27–31] (as shown in **Figure 5a, b**). This behavior is due to the competition between intermolecular and intramolecular hydrogen bonding below and above LCST



**Figure 4.**

(a) Schematic cross section of a liquid-based variable lens in a cylindrical glass housing (b) when a voltage is applied, charges accumulate in the wall electrode, and opposite charges collect near the solid/liquid interface in the conducting liquid. (c)–(e) Video frames of a 6-mm-diameter lens taken at voltages of 0, 100, and 120 V. Reproduced with permission from [24].



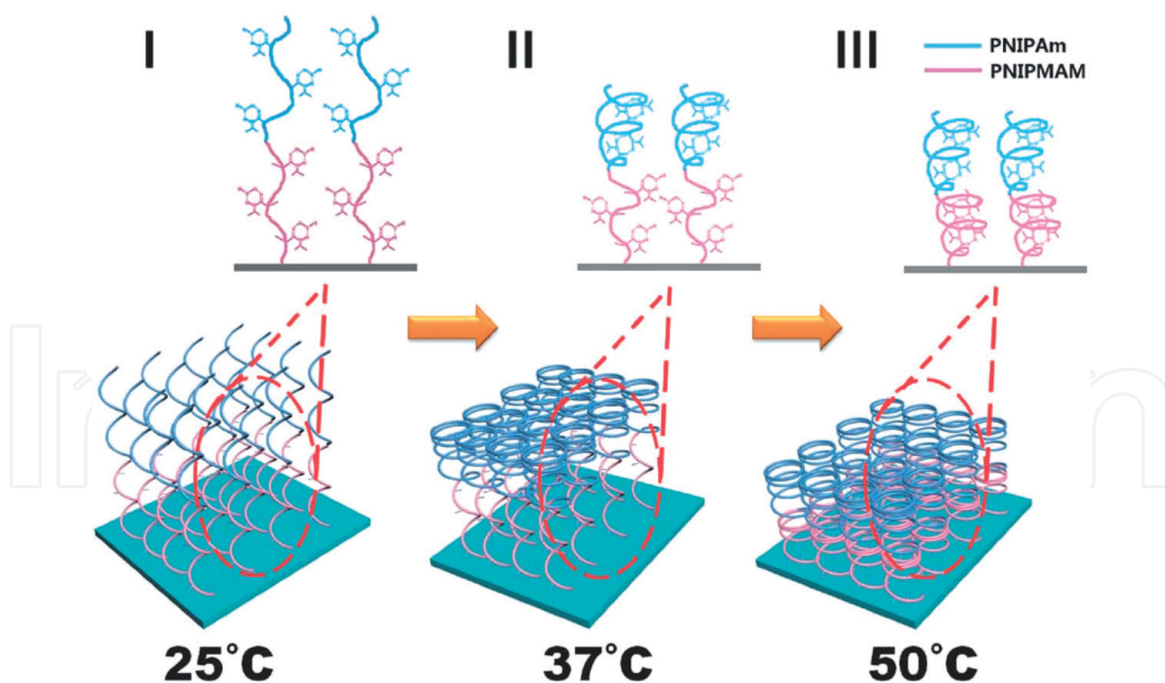


**Figure 5.**  
 (a) SEM image of the nanostructures on a rough substrate modified with PNIPAAm. (b) Water drop profile for the responsive surface at 25°C and 40°C. (c) Diagram of reversible formation of intermolecular hydrogen bonding between PNIPAAm chains and water molecules (left) and intramolecular hydrogen bonding between C=O and N-H groups in PNIPAAm chains (right) below and above the LCST. (d) Contact angles at two different temperatures 20 and 40°C for PNIPAAm-modified rough substrate. Reproduced with permission from [29].

(**Figure 5C**). The introduction of small surface roughness with a thermoresponsive coating dramatically improves the range of wettability. It makes it possible to get a switch of the wettability between the superhydrophobic and superhydrophilic states in a narrow temperature range. In the past decades, various other investigations reveal the progress in the direction of thermoresponsive surfaces to get the large wettability switch by combining surface features with PNIPAAm coating [28, 32].

Fu et al. reported a versatile approach to demonstrate the dynamical change of surface wettability by preparing nano-porous aluminum surfaces utilizing nanostructured surfaces modified with PNIPAAm coating [33]. Furthermore, a rough copper mesh film with hierarchical micro and nanostructures modified with PNIPAAm coating was used for temperature controlled water permeation [28]. For instance, micro/nanostructured composite films of PNIPAAm and polystyrene with controllable thermoresponsive wettability, which could switch between superhydrophobic and superhydrophilic was prepared by electrospinning technique [34]. Later by combining two thermoresponsive polymers poly(NIPAAm-co-NIPMAM), precise control over wettability switch from gradual to sudden could be achieved by precisely controlling the transition temperature [30]. Furthermore, low-cost block polymer brush containing poly(N-isopropylmethacrylamide)-block-poly(N-isopropylacrylamide) (PNIPMAM-b-PNIPAAm) was fabricated on the microstructured silicon substrate using ATRP technique, and multistage thermoresponsive wettability was observed. ATRP is an excellent method to construct block polymer brushes with different LCST on the surface. For instance, LCST of PNIPAAm and PNIPMAM is about 32 and 44° respectively. At temperature below 32 (LCST of PNIPAAm) PNIPMAM-b-PNIPAAm chains show loosely coiled molecular



**Figure 6.**

*Proposed principle of the constriction of PNIPMAM-*b*-PNIPAAm brushes with the increasing of temperature. Reproduced with permission from [32].*

arrangement and thus show hydrophilic behavior with a contact angle of  $20.9 \pm 2.8^\circ$ ; (as shown in **Figure 6—I**); when the temperature is raised beyond  $32^\circ$  but below  $44^\circ$ , PNIPAAm undergo phase change because it has crossed its LCST, which lead to form a collapsed and compact conformation of upper PNIPAAm chains induced by intramolecular hydrogen bonding and show less hydrophilic behavior with a contact angle of about  $85.2 \pm 2.7^\circ$  (**Figure 6—II**). Further increasing the temperature above  $44^\circ$  (LCST of PNIPAAm), the molecular arrangement of PNIPAAm chains would change, which would further collapse the polymer chains making the surface more hydrophobic with a contact angle of about  $108.6 \pm 2.1^\circ$  (**Figure 6—III**) [32]. Meanwhile, various other investigations have dealt with the fabrication of tunable wettability surfaces based on the polymer brush coating on cotton fabrics [35, 36].

Jiang et al. fabricated thermoresponsive co-polymer, PHFBMA-*b*-(PGMA-*g*-PNIPAM), by controlled free radical polymerization, which was used to fabricate a tunable wettability cotton fabric by dip-coating it into the thermoresponsive micelle. Dried cotton fabric was smooth with high fluorine content and showed hydrophobic behavior at low temperatures while at high temperatures; the surface of the cotton fabric was rough with low fluorine content and showed good hydrophilic behavior [36]. In addition to thermoresponsive polymers, which have been used extensively to fabricate the thermoresponsive surfaces, thermoresponsive inorganic oxides can also be used to get reversible thermoresponsive wetting transition [37, 38]. Due to the fast switching wettability in a narrow temperature range, thermoresponsive surfaces offer promising applications in areas including the thermally driven movement of liquid, oil–water separation, and switchable adhesion on the surface [39–44].

### 2.3 Photoresponsive surfaces

Surface wettability can be intelligently controlled using a variety of photoreponsive inorganic and organic oxides and polymers that are based on two main features: the switch of bi-stable states and change of surface free energy under light (electromagnetic radiation) stimulus. Surface wettability can be reversibly switched to a highly wetting state under ultraviolet (UV) illumination, and the original state

is recovered after the surface is placed for a longer time period in dark and/or heated at elevated temperature. Among various photoresponsive materials, inorganic oxides (wide bandgap semiconducting material) are widely used in various applications owing to their excellent chemical and mechanical stability, low cost, and outstanding optoelectronic properties. Among the different photosensitive inorganic materials, titanium dioxide ( $\text{TiO}_2$ ) and zinc oxide ( $\text{ZnO}$ ) are the most common semiconductors widely used for their excellent UV absorption characteristics as their bandgap corresponds to the UV energy. The mechanism involving photogeneration of electron and holes and absorption of water is responsible for the change in the wettability. Photoresponsive wettability change of titanium dioxide was first reported by Wang et al. [45] and later discussed in detail by Pant et al. [46]. They have shown that the wetting behavior on a surface coated with a polycrystalline thin film of  $\text{TiO}_2$  could be reversibly switched between the hydrophilic and hydrophobic states under UV irradiation and dark storage. Respective hydrophilic behavior is due to the conversion of  $\text{Ti}^{4+}$  state to  $\text{Ti}^{3+}$  state under UV illumination. For practical applications, it is highly desirable to get the surfaces with wettability switching in a large range from superhydrophobic to superhydrophilic states, which can be obtained by combining the surface roughness with a photoresponsive smart material coating of desired surface chemistry. Introduction of fine nano roughness enhances the hydrophilic and hydrophobic performances. By introducing nanoscale roughness, Tadanaga et al. demonstrated the reversible wetting transition by UV irradiation on a superhydrophobic surface with three layers: flowerlike  $\text{Al}_2\text{O}_3$ , thin  $\text{TiO}_2$  gel, and fluoroalkylsilane [47]. Later Feng et al. reported similar reversible wettability switch between superhydrophobic and superhydrophilic states of  $\text{ZnO}$  nanorod films, as shown in Figure 7a–d [48].

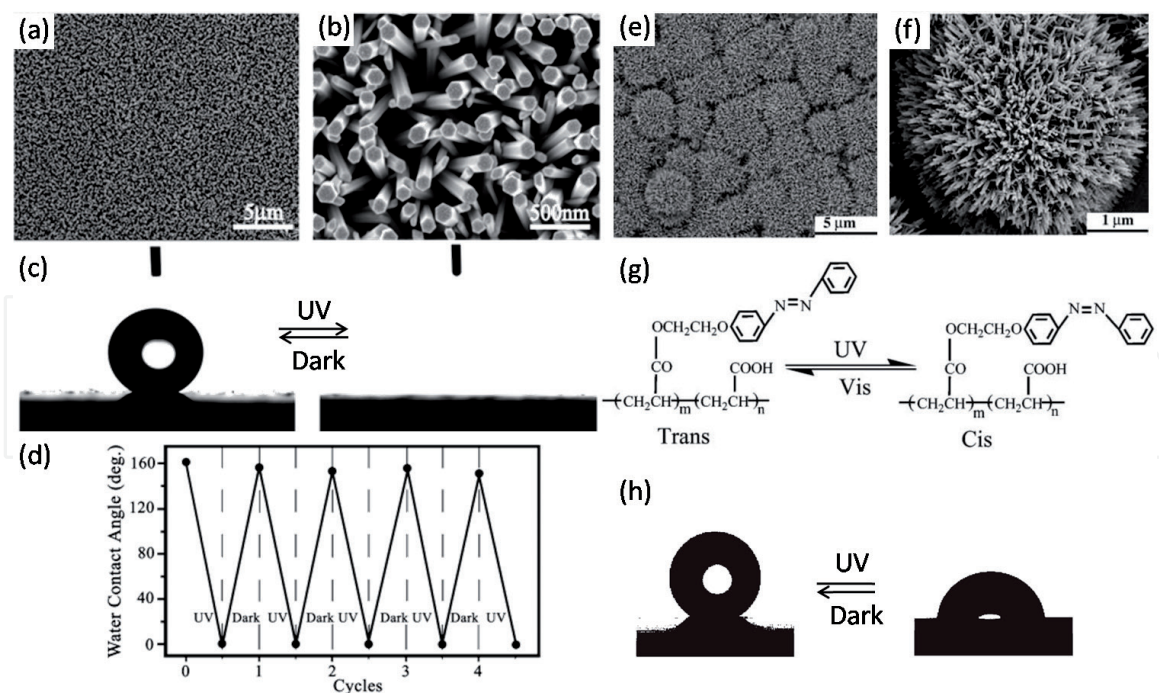


**Figure 7.** (a, b) FE-SEM top-images of the as-prepared  $\text{ZnO}$  nanorod films at low and high magnifications, respectively. (c) Photographs of water droplet shape on the aligned  $\text{ZnO}$  nanorod films before (left) and after (right) UV illumination, reproduced with permission from [48]. (d) Reversible superhydrophobic to superhydrophilic transition of the as-prepared films under the alternation of UV irradiation and dark storage. (e) Low-magnification FE-SEM image of a  $\text{TiO}_2$  nanorod film deposited on a glass wafer; (f) morphology of a single papilla at high magnification, reproduced with permission from [49]. (g) The trans and cis structures of azobenzene upon UV and Vis irradiation. (h) The shapes of water drop on photoresponsive monolayer with a patterned substrate of 40-mm pillar spacing upon UV and Vis irradiation. Reproduced with permission from [50].

They reported that UV irradiation would lead to generate electron-hole pairs and form oxygen vacancies on the surface. Competition between water and oxygen will decide which component will absorb the oxygen vacancies on the surface. Surface hydrophilicity is a cause of the adsorption of hydroxyl groups on the surface; however this state is energetically unstable. Therefore, the hydroxyl groups adsorbed on the surface are replaced by the oxygen groups (which is thermodynamically more stable) after the UV-irradiated surfaces are placed in dark and subsequently, the surface reverts to its original state and the wettability switches from superhydrophobic to superhydrophilic. Further, by introducing micro and nanoscale hierarchical surface structures, Feng et al. showed the reversible wetting switching between superhydrophilic and superhydrophobic states on TiO<sub>2</sub> nanorod films by cooperating micro and nano hierarchical surface structures together with a photosensitive material coating and the wettability change was quite similar to as reported in their previous work [49]. Morphology of hierarchical surface structures with micro and nano features can be clearly visualized from the SEM images shown in **Figure 7e, f**. Due to intrinsic photocatalytic property and reversible wettability switch, TiO<sub>2</sub> has also attracted much attention for its various applications, such as antifogging and self-cleaning [51–55]. Another simple approach to produce rough TiO<sub>2</sub> films was based on CF<sub>4</sub> plasma etching technique, which was adopted by Zhang et al. to produce superhydrophilic and superhydrophobic patterns by UV irradiation using a photomask [56]. However, rough surfaces often lead to scattering of light due to the level of the roughness being larger than the wavelength of visible light. This problem can be addressed by reducing the level of roughness to a scale comparable to the wavelength of the visible light [57]. In addition to TiO<sub>2</sub>, other inorganic photoresponsive wide bandgap semiconductor materials such as ZnO, SnO<sub>2</sub>, V<sub>2</sub>O<sub>5</sub>, WO<sub>3</sub> etc. are also used to get the reversible wettability switch between two extreme states [48, 56, 58, 59]. To achieve different functions such as transparency and conductivity, SnO<sub>2</sub> conducting nanorods were prepared, showing 60% transmittance in the visible range, which can meet the demand of smart microfluidic devices [58]. In addition, tungsten oxide films prepared by the electrochemical deposition method demonstrate dual responsive wettability switch and photochromatic characteristics [60].

In addition to inorganic materials, various organic compounds/polymers with stimuli-responsive properties and a reversible photoinduced transformation between two states have been widely used. The various photoresponsive functional groups include azobenzenes, pyrimidines, spiropyran, cinnamates etc. Responsive surface wettability change is associated with the change in the surface free energy caused by the change in chemical composition upon UV irradiation. Among various organic compounds, azobenzene is the most promising photoresponsive material, whose molecular structure reversible transits between trans and cis states under visible and UV illumination [61]. Azobenzene layer with a trans isomer state possesses a larger water contact angle, which is governed by the small dipole moment and low surface energy, while cis state exhibits small contact angle due to high dipole moment and large surface energy. Reversible wettability change from superhydrophobic to superhydrophilic is associated with the corresponding change of state from trans isomer to cis isomer under UV and visible illumination (**Figure 7g**). Using a simple electrostatic self-assembly technique, Jiang et al. showed photo switched wettability on organic azobenzene monolayer with a large reversible change of contact angle (**Figure 7h**) [50]. Since then, various other research groups have worked on the preparation of tunable wetting surfaces based on the photoresponsive organic materials and subsequent manipulation of the wettability via controlling surface properties by irradiating UV light [62–64]. Because of the unique properties of these photoresponsive polymers, they are widely used in various



applications such as antifogging, self-cleaning, adhesion control, liquid printing, and oil–water separation [52, 53, 65–67]. Photoresponsive surfaces have also gained much attention in biomedical areas utilizing the light-responsive controlled release system where a guest molecule could be released from the surface in a controlled manner by adjusting the wetting behavior of the surface.

Chen et al. realized a light-responsive release system by controlling the wetting behavior of mesoporous (MS) silica surface-functionalized with an optimal ratio of spiropyran mixed with fluorosilane [67]. They reported that, under UV irradiation (365 nm), the surface could be wetted by water due to the conversion of spiropyran molecule from closed-form to open-form, which resulted in the switch of wettability from hydrophobic to hydrophilic state and release of cargo molecules from the pores (Figure 8).

## 2.4 Mechanically tunable surfaces

As it is mentioned earlier, the surface wettability is mainly governed by chemical composition and structures of the surface. Altering one of these factors would lead to change the surface wetting properties. Most of the external stimulus changes the chemical composition of the substrate; however, changing the surface structures also produces a change in the surface wettability. Various research groups have demonstrated the mechanical stress-responsive tunable wettability using elastic or gel materials [68–75]. Poly(tetrafluoroethylene) PTFE is the most common

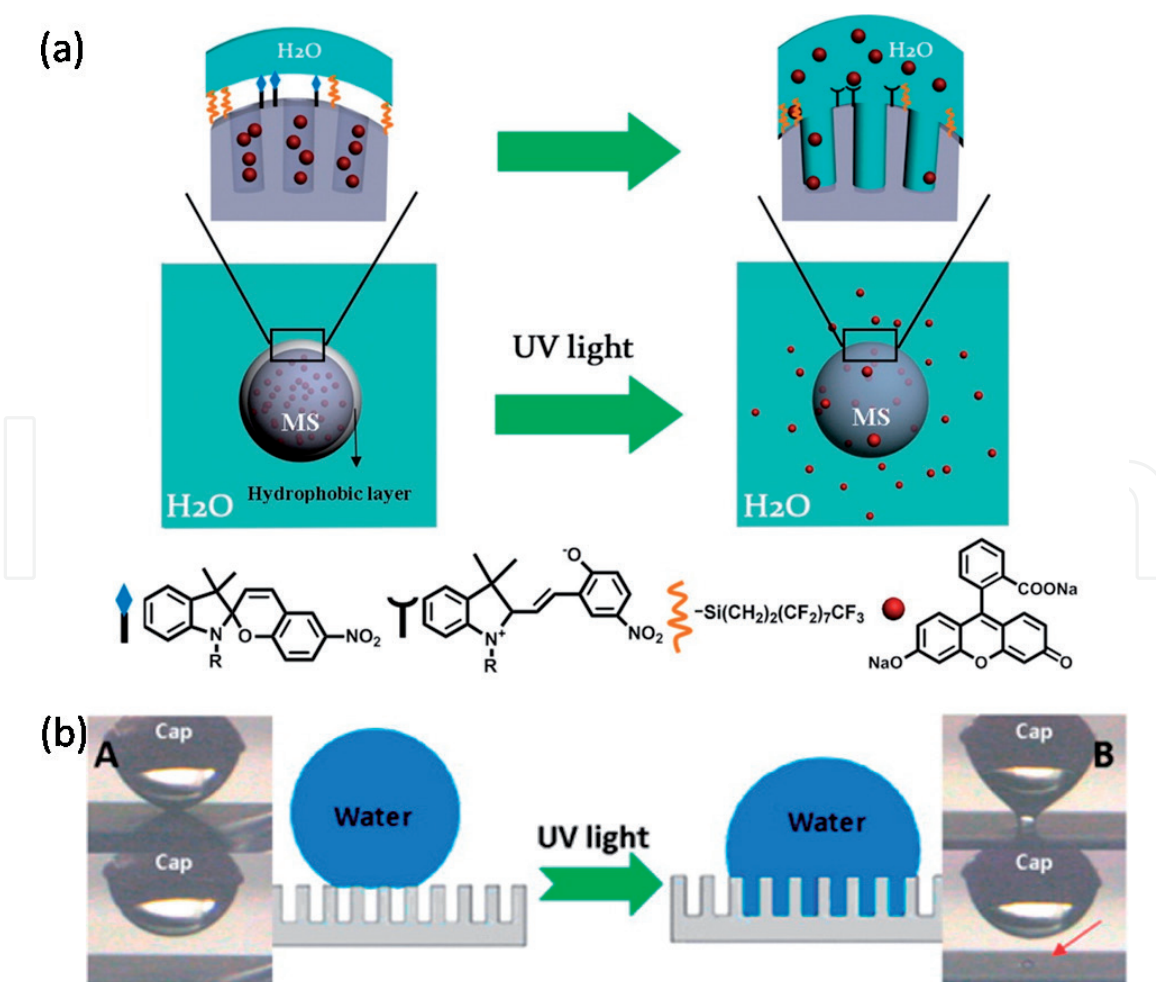


**Figure 8.**  
 (a) The schematic of the light-responsive release system. After irradiation with 365 nm UV light, the surface became wet due to the conformational conversion of spiropyran from the “closed” form to the “open” form (b). The mechanism illustrating the wetting process of surface. Reproduced with permission from [67].

hydrophobic material, and Teflon tape, made with PTFE crystals, has been widely used to tune the wetting behavior by applying mechanical strain. Zhang et al. demonstrated a change in the density of PTFE crystal by axial extension [68]. They also reported that with an extension of the PTFE crystals to 190%, water contact angle could be tuned between hydrophobic ( $118^\circ$ ) and superhydrophobic ( $165^\circ$ ) states. In their next work, using this approach of biaxial extension and unloading, they have shown reversible wettability switch between superhydrophilic and superhydrophobic behavior of the polyamide films with triangular structures [69]. Initially the polyamide film with the triangular structures showed superhydrophobic behavior with a water contact angle of  $\sim 151.2^\circ$ . When the film is extended to 120%, water penetrates through space among the fiber resulting in the complete wetting situation. While unloading, the polyamide film returned to the superhydrophobic state due to the recovery of the surface structures. In addition, poly(dimethylsiloxane) (PDMS) microwrinkle structures also demonstrate tunable wetting behavior upon stretching. Wrinkling approach is very useful as its wavelength and amplitude can be actively tuned to produce various well-defined structures.

Lin et al. have shown the fabrication of superhydrophobic surface, featured with micro and nanoscale roughness, using nanoparticle coating on PDMS wrinkled structures [71]. For the first time, they have shown the fabrication of a superhydrophobic surface by combining microstructured PDMS wrinkles with nanoparticles. **Figure 9** is a schematic illustration of the fabrication of PDMS elastic film with dual scale roughness. Surface topography can be reversibly tuned between complete relaxed state (wrinkle formation) and the complete stretched state (only nano roughness), that is, reversible switching between the dual scale roughness and nanoscale roughness (as shown in **Figure 9f–k**). Using both theoretical and

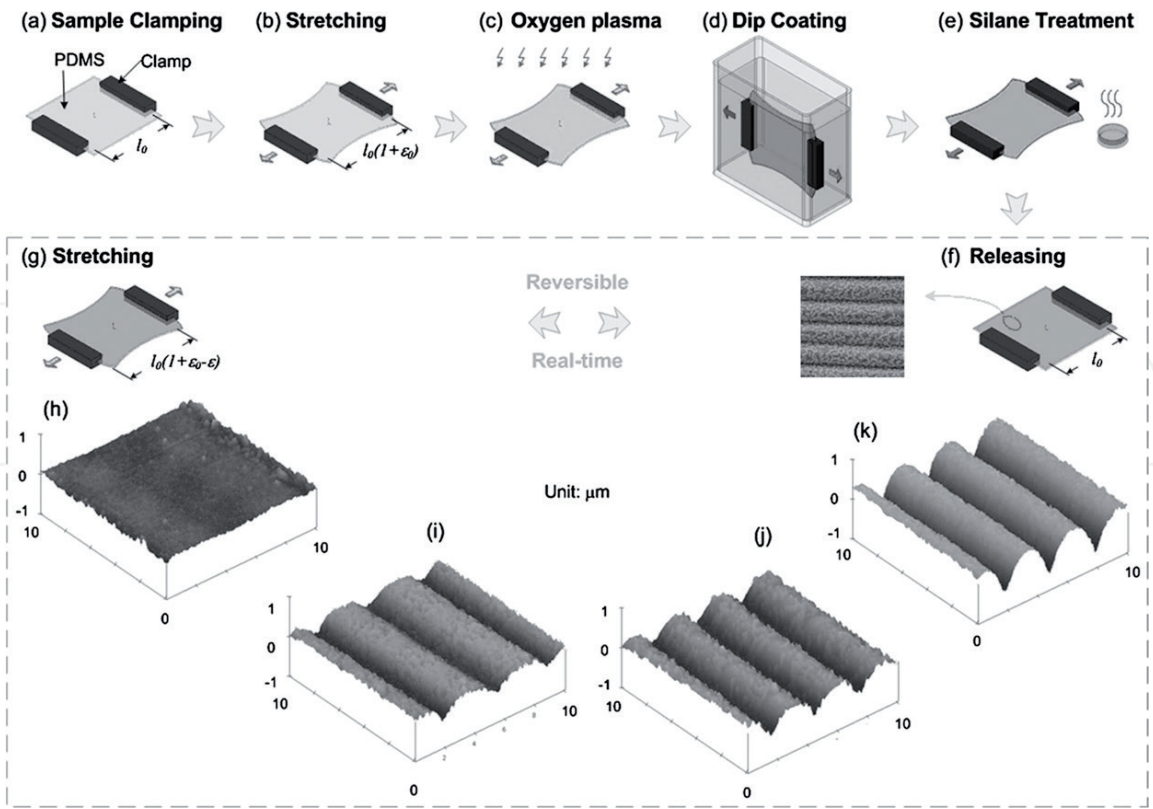


**Figure 9.** A schematic illustration of the fabrication of a PDMS film with dual-scale roughness (a–f) and real-time, reversible tunability of its surface topography by mechanical strain (f–k). Inset shows the optical images of a water drop on the surface with dual-scale roughness (right) and nanoscale roughness (left). Reproduced with permission from [71].

experimental approaches, they concluded that only micron-scale roughness is not able to attain Cassie-Baxter state. By regulating the surface topography by applying different mechanical strain, they have shown switching between different wetting states from Cassie-Baxter (dual scale roughness) to Wenzel (both micron wrinkle and nanoparticle-coated elastic film). Chung et al. have shown that the drop shape strongly gets affected by the geometrical anisotropy of the sinusoidal grooves as on the isotropic surface contact angle were uniquely defined; however this was not the case for anisotropic surfaces on which drop showed two different contact angles in the direction parallel and perpendicular to the grooves [70].

## 2.5 pH-responsive surfaces

In recent years, pH-responsive wetting has gained a lot of attention because of their emerging applications in various fields such as drug delivery and biosensors [76]. It is of particular interest where it is required to change the wetting behavior of various acidic and basic liquids. Xu et al. have shown a novel method to prepare pH-responsive surfaces containing block copolymer thin films of poly(styrene-*b*-acrylic acid) (PS-*b*-PAA) and pH-responsive nanostructures composed of cylindrical domains [77]. PS-*b*-PAA polymer films show different surface morphologies for three different pH regimes. These polymers films swell more rapidly when immersed in high-pH solutions compared to low-pH solutions. They also observed that with the increase in the pH from 2.6 to 9.1, the water contact angle decreased by 30°. The decrease in the contact angle is due to the rear molecular arrangement of PAA chains in response to increase in pH, which results in increasing hydrophilicity [77, 78]. They concluded that wettability can be regulated by controlling the molecular arrangement of PAA chains in response to pH stimulus.

Uhlmann et al. introduced the idea of surface functionalization for the smart coatings using stimuli-responsive binary polymer brushes containing polymer chains of two different polymers using “grafting from” and “grafting to” approach [79]. The concept of reversible switching can be understood based on the reaction of polymers with different solvents, where a polymer brush of hydrophilic and hydrophobic polymers is treated with nonselective and selective solvents for both the polymers. In a good solvent, due to the dominance of the interchain repulsion, polymer chains show stretched conformation while in a bad solvent, due to strong repulsion between solvent and polymer, chains show coiled and collapsed conformation. This can also be interpreted as; brush structure shows hydrophilic behavior when treated with a selective solvent for polymer A while shows hydrophobic behavior when treated with a selective solvent for polymer B. However, in a nonselective solvent, both polymers show laterally segregate structures. Later Lu et al. reported a system of layer by layer (LbL) hydrogels, composed of amphiphilic polymers, which can undergo a reversible transition in response to pH stimulus. To shed light on the exact wetting state of hydrophobic PaAALbL-coated patterned surface, they measured the CAH (**Figure 10A**) and imaged the behavior of a water drop for different pH values (**Figure 10B–E**). For  $\text{pH} < 6$ , contact angle hysteresis was too large, close to 120° and the drop was sticky to the surface, and did not fall even if the substrate was turned vertically down. Such stickiness behavior with high CAH is realized for the drop in the Wenzel state, and the observed behavior can be accounted for the enhanced contact line pinning by the surface microstructures [80]. Numerous other researchers have also investigated pH-responsive tunable wetting behavior from its fundamental understanding of switchable wettability [78, 81–83].



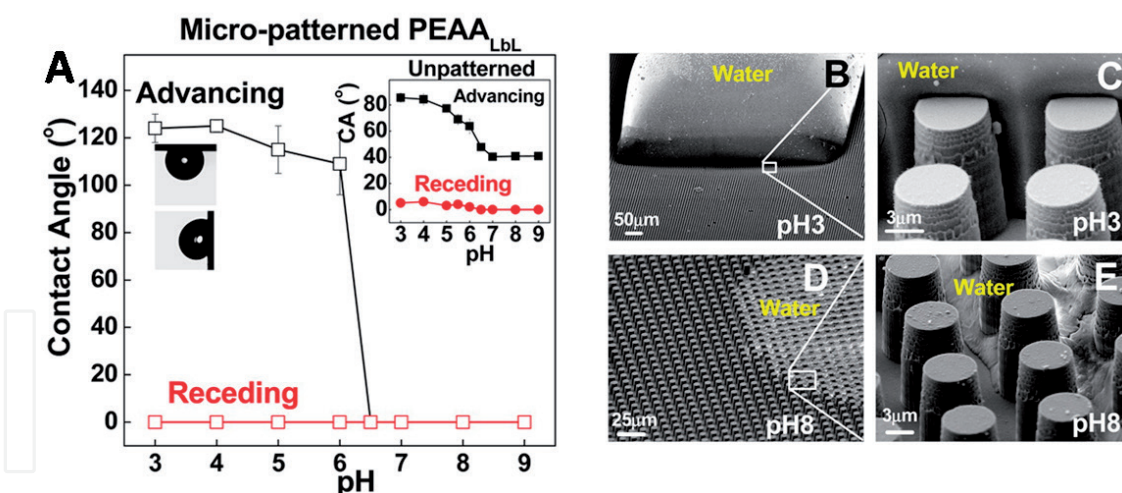


**Figure 10.**

(A) Advancing and receding CAs of PEAA<sub>LbL</sub> on a micro-patterned substrate with a square array of cylindrical pillar structures. Optical images show water droplets sticking to the substrate at pH 3, suggesting strong pinning. Inset in the upper right corner represents advancing and receding CAs of water droplets on the unpatterned substrate. (B–E) Cryo-SEM images of a water droplet on a PEAA<sub>LbL</sub>-coated micropillar-patterned substrate at (B, C) pH 3 and (D, E) pH 8. Reproduced with permission from [80].

## 2.6 Other stimuli

Some of the recent work also demonstrates using magnetic field and solvents as external stimuli to manipulate the wettability for given fluids. Smart surfaces that respond to magnetic field have been demonstrated by numerous research groups in the last decade [84, 85]. Grigoryev et al. fabricated a microstructured surface with reentrant geometry composed of Ni micronails, which shows a reversible transition from superomniphobic to omniphilic wetting state in response to the external magnetic field [85]. Cheng et al. also showed the reversible wetting transitions of the microdroplet consisting of superparamagnetic Fe<sub>3</sub>O<sub>4</sub> nanoparticles [84]. They have shown that the wettability can be reversibly switched between the Cassie state and the Wenzel state on the microstructured silicon substrate and the transition between two wetting states can be controlled by both concentration of nanoparticles and the intensity of the magnetic field. On the other hand, solvent as an external stimulus is also feasible to tune the wetting behavior as solvent-responsive surfaces are affected by the surrounding medium and their wettability change is governed by the change in their interfacial energy caused by the rearrangement of the molecular chains in response to a solvent [81, 86–88]. Minko et al. demonstrated a novel route to fabricate two-level structured polymer brushes, and the surface wettability could be reversibly controlled by exposing the polymer brush surfaces to the solvent, which is selective to one of the polymers. Surface morphology and surface properties change when exposed to different solvents, which is caused by the interchange between vertical and linear phase segregation of the polymers [81].

## 3. Conclusions

To conclude, smart surfaces with tunable wettability based on various external stimulus prove to be useful candidates in different applications where the continuous and reversible tuning of surface wettability is important. These surfaces exploit the additional energy gained from the external stimulus to change their wetting behavior as per the requirement. It has been demonstrated that the surface wettability can be varied from hydrophobic to hydrophilic on smooth surfaces and from

superhydrophobic to superhydrophobic on patterned surfaces. Many such external stimuli are available to alter the surface wettability because each technique has few advantages and disadvantages over others. As described in different sections, almost complete understanding about most of the techniques has been established. Of course, there are some limiting cases where the scientific understanding is not completely clear and is an active area of research currently. Hence, depending upon the feasibility and available resources, users can choose a suitable stimulus for their application.

## Acknowledgements

The authors acknowledge fruitful discussion with Reeta Pant and Subhash Singha, which was particularly useful for the section “**Photoresponsive surfaces**”.

## Conflict of interest


The authors declare no conflict of interest.

## Author details

Meenaxi Sharma and Krishnacharya Khare\*  
Department of Physics, Indian Institute of Technology Kanpur, Kanpur, India

\*Address all correspondence to: [kcharya@iitk.ac.in](mailto:kcharya@iitk.ac.in)

## IntechOpen

© 2020 The Author(s). Licensee IntechOpen. This chapter is distributed under the terms of the Creative Commons Attribution License (<http://creativecommons.org/licenses/by/3.0>), which permits unrestricted use, distribution, and reproduction in any medium, provided the original work is properly cited. 

## References

- [1] Young T. An essay on the cohesion of fluids. Philosophical Transactions. Royal Society of London. 1805;**95**:65-87
- [2] Wenzel RN. Resistance of solid surfaces to wetting by water. Industrial and Engineering Chemistry. 1936;**28**(8):988-994
- [3] Cassie ABD, Baxter S. Wettability of porous surfaces. Transactions of the Faraday Society. 1944;**40**:546-551
- [4] Gabriel L. Relations entre les phénomènes électriques et capillaires. Annales de Chimie Physique. 1875;**5**:494
- [5] Mugele F, Baret J-C. Electrowetting: From basics to applications. Journal of Physics. Condensed Matter. 2005;**17**:R705-RR74
- [6] Nakamura Y, Matsumoto M, Nishizawa K, Kamada KI, Watanabe A. Studies on secondary electrocapillary effects: II. The electrocapillary phenomena in thin liquid film. Journal of Colloid and Interface Science. 1977;**59**(2):201-210
- [7] Berge B. Electrocapilarity and wetting of insulator film by water. Comptes Rendus de l'Academie des Sciences Serie II. 1993;**317**:157-163
- [8] Khare K, Herminghaus S, Baret J-C, Law BM, Brinkmann M, Seemann R. Switching liquid morphologies on linear grooves. Langmuir. 2007;**23**(26):12997-13006
- [9] Krupenkin TN, Taylor JA, Schneider TM, Yang S, et al. Langmuir. 2004;**20**(10):3824
- [10] Krupenkin TN, Taylor JA, Wang EN, Kolodner P, Hodes M, Salamon TR. Reversible wetting–dewetting transitions on electrically tunable Superhydrophobic nanostructured surfaces. Langmuir. 2007;**23**(18):9128-9133
- [11] Bormashenko E, Pogreb R, Balter S, Aurbach D. Electrically controlled membranes exploiting Cassie-Wenzel wetting transitions. Scientific Reports. 2013;**3**(1):3028
- [12] McHale G, Brown CV, Sampara N. Voltage-induced spreading and superspreading of liquids. Nature Communications. 2013;**4**(1):1605
- [13] Lokanathan M, Sharma H, Shabaka M, Mohanty K, Bahadur VJC, Physicochemical SA, et al. Comparing electrowettability and surfactants as tools for wettability enhancement on a hydrophobic surface. Colloids and Surfaces, A: Physicochemical and Engineering Aspects. 2020;**585**:124155
- [14] Mazuruk K, MP V. Electric field effect on the contact angle for non-wetting drops. Journal of Physics: Condensed Matter. 2019;**31**(39):395002
- [15] Teng P, Tian D, Fu H, Wang SJMCF. Recent progress of electrowetting for droplet manipulation: From wetting to superwetting systems. Materials Chemistry Frontiers. 2020;**4**(1): 140-154
- [16] Li F, Mugele F. How to make sticky surfaces slippery: Contact angle hysteresis in electrowetting with alternating voltage. Applied Physics Letters. 2008;**92**(24):244108
- [17] Maillard M, Legrand J, Berge B. Two liquids wetting and low hysteresis electrowetting on dielectric applications. Langmuir. 2009;**25**(11):6162-6167
- [18] de Ruiter R, Semperebon C, van Gorcum M, Duits MHG, Brinkmann M, Mugele F. Stability limits of capillary bridges: How contact angle hysteresis affects morphology transitions of liquid microstructures. Physical Review Letters. 2015;**114**(23):234501



- [19] Bormashenko E, Pogreb R, Bormashenko Y, Grynyov R, Gendelman O. Low voltage reversible electrowetting exploiting lubricated polymer honeycomb substrates. *Applied Physics Letters*. 2014;**104**(17):171601
- [20] Hao C, Liu Y, Chen X, He Y, Li Q, Li KY, et al. Electrowetting on liquid-infused film (EWOLF): Complete reversibility and controlled droplet oscillation suppression for fast optical imaging. *Scientific Reports*; **4**:2014, 6846
- [21] Barman J, Pant R, Nagarajan AK, Khare K. Electrowetting on dielectrics on lubricating fluid-infused smooth/rough surfaces with negligible hysteresis. *Journal of Adhesion Science and Technology*. 2017;**31**(2):159-170
- [22] Bormashenko E, Pogreb R, Bormashenko Y, Aharoni H, Shulzinger E, Grinev R, et al. Progress in low voltage reversible electrowetting with lubricated polymer honeycomb substrates. *RSC Advances*. 2015;**5**(41):32491-32496
- [23] Berge B, Peseux J. Variable focal lens controlled by an external voltage: An application of electrowetting. *European Physical Journal E: Soft Matter and Biological Physics*. 2000;**3**(2):159-163
- [24] Kuiper S, Hendriks BHW. Variable-focus liquid lens for miniature cameras. *Applied Physics Letters*. 2004;**85**(7):1128
- [25] Hayes RA, Feenstra BJ. Video-speed electronic paper based on electrowetting. *Nature*. 2003;**425**(6956):383
- [26] Wischerhoff E, Zacher T, Laschewsky A, Rekaï ED. Direct observation of the lower critical solution temperature of surface-attached thermo-responsive hydrogels by surface plasmon resonance. *Angewandte Chemie, International Edition*. 2000;**39**(24):4602-4604
- [27] Sun T, Wang G, Feng L, Liu B, Ma Y, Jiang L, et al. Reversible switching between superhydrophilicity and superhydrophobicity. *Angewandte Chemie, International Edition*. 2004;**43**(3):357-360
- [28] Song W, Xia F, Bai Y, Liu F, Sun T, Jiang L. Controllable water permeation on a poly(N-isopropylacrylamide)-modified nanostructured copper mesh film. *Langmuir*. 2007;**23**(1):327-331
- [29] Xia F, Zhu Y, Feng L, Jiang L. Smart responsive surfaces switching reversibly between super-hydrophobicity and super-hydrophilicity. *Soft Matter*. 2009;**5**(2):275-281
- [30] Zhao T, Nie F-Q, Jiang L. Precise control of wettability from LCST tunable surface. *Journal of Materials Chemistry*. 2010;**20**(11):2176-2181
- [31] Konosu Y, Matsumoto H, Tsuboi K, Minagawa M, Tanioka A. Enhancing the effect of the nanofiber network structure on thermoresponsive wettability switching. *Langmuir*. 2011;**27**(24):14716-14720
- [32] Song W, Li H, Wang C, Yang B. Design of multi-stage thermal responsive wettable surface. *Advanced Materials Interfaces*. 2014;**1**(6):1400009
- [33] Fu Q, Rama Rao GV, Basame SB, Keller DJ, Artyushkova K, Fulghum JE, et al. Reversible control of free energy and topography of nanostructured surfaces. *Journal of the American Chemical Society*. 2004;**126**(29):8904-8905
- [34] Wang N, Zhao Y, Jiang L. Low-cost, thermoresponsive wettability of surfaces: Poly(N-isopropylacrylamide)/ polystyrene composite films prepared by electrospinning. *Macromolecular Rapid Communications*. 2008;**29**:485-489

- [35] Jiang B, Zhang L, Liao B, Pang H. Self-assembly of well-defined thermo-responsive fluoropolymer and its application in tunable wettability surface. *Polymer*. 2014;**55**(21):5350-5357
- [36] Jiang B, Pang H. Synthesis and self-assembly of thermoresponsive block-graft fluoropolymer as well as its tunable wettability surface. *Journal of Polymer Science, Part A: Polymer Chemistry*. 2016;**54**(7):992-1002
- [37] Yang J, Zhang Z, Men X, Xu X, Zhu X. Thermo-responsive surface wettability on a pristine carbon nanotube film. *Carbon*. 2011;**49**(1):19-23
- [38] Zhang M, Yao G, Cheng Y, Xu Y, Yang L, Lv J, et al. Temperature-dependent differences in wettability and photocatalysis of TiO<sub>2</sub> nanotube arrays thin films. *Applied Surface Science*. 2015;**356**:546-552
- [39] Li C, Guo R, Jiang X, Hu S, Li L, Cao X, et al. Reversible switching of water-droplet mobility on a superhydrophobic surface based on a phase transition of a side-chain liquid-crystal polymer. *Advanced Materials*. 2009;**21**(42):4254-4258
- [40] Wang T, Chen H, Liu K, Wang S, Xue P, Yu Y, et al. Janus Si micropillar arrays with thermal-responsive anisotropic wettability for manipulation of microfluid motions. *ACS Applied Materials & Interfaces*. 2015;**7**(1):376-382
- [41] Wang Y, Lai C, Hu H, Liu Y, Fei B, Xin JH. Temperature-responsive nanofibers for controllable oil/water separation. *RSC Advances*. 2015;**5**(63):51078-51085
- [42] Li J-J, Zhu L-T, Luo Z-H. Electrospun fibrous membrane with enhanced switchable oil/water wettability for oily water separation. *Chemical Engineering Journal*. 2016;**287**:474-481
- [43] Frysali MA, Anastasiadis SHJL. Temperature-and/or pH-responsive surfaces with controllable wettability: From parahydrophobicity to superhydrophilicity. *Langmuir*. 2017;**33**(36):9106-9114
- [44] Li X, Jiang Y, Jiang Z, Li Y, Wen C, Lian JJASS. Reversible wettability transition between superhydrophilicity and superhydrophobicity through alternate heating-reheating cycle on laser-ablated brass surface. *Applied Surface Science*. 2019;**492**:349-361
- [45] Wang R, Hashimoto K, Fujishima A, Chikuni M, Kojima E, Kitamura A, et al. Light-induced amphiphilic surfaces. *Nature*. 1997;**388**(6641):431-432
- [46] Pant R, Singha S, Bandyopadhyay A, Khare K. Investigation of static and dynamic wetting transitions of UV responsive tunable wetting surfaces. *Applied Surface Science*. 2014;**292**:777-781
- [47] Tadanaga K, Morinaga J, Matsuda A, Minami T. Superhydrophobic–superhydrophilic micropatterning on flowerlike alumina coating film by the sol–gel method. *Chemistry of Materials*. 2000;**12**(3):590-592
- [48] Feng X, Feng L, Jin M, Zhai J, Jiang L, Zhu D. Reversible superhydrophobicity to superhydrophilicity transition of aligned ZnO nanorod films. *Journal of the American Chemical Society*. 2004;**126**(1):62-63
- [49] Feng X, Zhai J, Jiang L. The fabrication and switchable superhydrophobicity of TiO<sub>2</sub> nanorod films. *Angewandte Chemie, International Edition*. 2005;**44**(32):5115-5118
- [50] Jiang W, Wang G, He Y, Wang X, An Y, Song Y, et al. Photo-switched wettability on an electrostatic self-assembly azobenzene monolayer. *Chemical Communications*. 2005;**28**:3550-3552

- [51] Zhang X-T, Sato O, Taguchi M, Einaga Y, Murakami T, Fujishima A. Self-cleaning particle coating with antireflection properties. *Chemistry of Materials*. 2005;17(3):696-700
- [52] Cebeci FÇ, Wu Z, Zhai L, Cohen RE, Rubner MF. Nanoporosity-driven superhydrophilicity: A means to create multifunctional antifogging coatings. *Langmuir*. 2006;22(6):2856-2862
- [53] Zhang L, Dillert R, Bahnemann D, Vormoor M. Photo-induced hydrophilicity and self-cleaning: Models and reality. *Energy & Environmental Science*. 2012;5(6):7491-7507
- [54] Nau M, Seelinger D, Biesalski M. Independent two way switching of the wetting behavior of cellulose-derived nanoparticle surface coatings by light and by temperature. *Advanced Materials Interfaces*. 2019;6(17):1900378
- [55] Shami Z, Holakooei P. Durable light-driven three-dimensional smart switchable superwetting nanotextile as a green scaled-up oil–water separation technology. *ACS Omega*. 2020;5(10):4962-4972
- [56] Zhang X, Jin M, Liu Z, Tryk DA, Nishimoto S, Murakami T, et al. Superhydrophobic TiO<sub>2</sub> surfaces: Preparation, photocatalytic wettability conversion, and superhydrophobic–superhydrophilic patterning. *Journal of Physical Chemistry C*. 2007;111(39):14521-14529
- [57] Zhang X, Kono H, Liu Z, Nishimoto S, Tryk DA, Murakami T, et al. A transparent and photo-patternable superhydrophobic film. *Chemical Communications*. 2007;46:4949-4951
- [58] Zhu W, Feng X, Feng L, Jiang L. UV-manipulated wettability between superhydrophobicity and superhydrophilicity on a transparent and conductive SnO<sub>2</sub> nanorod film. *Chemical Communications*. 2006;26:2753-2755
- [59] Wang S, Song Y, Jiang L. Photoresponsive surfaces with controllable wettability. *Journal of Photochemistry and Photobiology, C: Photochemistry Reviews*. 2007;8(1):18-29
- [60] Wang S, Feng X, Yao J, Jiang L. Controlling wettability and photochromism in a dual-responsive tungsten oxide film. *Angewandte Chemie, International Edition*. 2006;45(8):1264-1267
- [61] Pan S, Ni M, Mu B, Li Q, Hu X-Y, Lin C, et al. Well-defined pillararene-based azobenzene liquid crystalline photoresponsive materials and their thin films with photomodulated surfaces. *Advanced Functional Materials*. 2015;25(23):3571-3580
- [62] Ge H, Wang G, He Y, Wang X, Song Y, Jiang L, et al. Photoswitched wettability on inverse opal modified by a self-assembled azobenzene monolayer. *ChemPhysChem*. 2006;7(3):575-578
- [63] Blasco E, Piñol M, Oriol L, Schmidt BVKJ, Welle A, Trouillet V, et al. Photochemical generation of light responsive surfaces. *Advanced Functional Materials*. 2013;23(32):4011-4019
- [64] Takase K, Hyodo K, Morimoto M, Kojima Y, Mayama H, Yokojima S, et al. Photoinduced reversible formation of a superhydrophilic surface by crystal growth of diarylethene. *Chemical Communications*. 2016;52(42):6885-6887
- [65] Lim HS, Han JT, Kwak D, Jin M, Cho K. Photoreversibly switchable superhydrophobic surface with erasable and rewritable pattern. *Journal of the American Chemical Society*. 2006;128(45):14458-14459



- [66] Tian D, Zhang X, Tian Y, Wu Y, Wang X, Zhai J, et al. Photo-induced water–oil separation based on switchable superhydrophobicity–superhydrophilicity and underwater superoleophobicity of the aligned ZnO nanorod array-coated mesh films. *Journal of Materials Chemistry*. 2012;**22**(37):19652-19657
- [67] Chen L, Wang W, Su B, Wen Y, Li C, Zhou Y, et al. A light-responsive release platform by controlling the wetting behavior of hydrophobic surface. *ACS Nano*. 2014;**8**(1):744-751
- [68] Zhang J, Li J, Han Y. Superhydrophobic PTFE surfaces by extension. *Macromolecular Rapid Communications*. 2004;**25**(11):1105-1108
- [69] Zhang J, Lu X, Huang W, Han Y. Reversible superhydrophobicity to superhydrophilicity transition by extending and unloading an elastic polyamide film. *Macromolecular Rapid Communications*. 2005;**26**(6): 477-480
- [70] Chung JY, Youngblood JP, Stafford CM. Anisotropic wetting on tunable micro-wrinkled surfaces. *Soft Matter*. 2007;**3**(9):1163-1169
- [71] Lin P-C, Yang S. Mechanically switchable wetting on wrinkled elastomers with dual-scale roughness. *Soft Matter*. 2009;**5**(5):1011-1018
- [72] Yang S, Khare K, Lin P-C. Harnessing surface wrinkle patterns in soft matter. *Advanced Functional Materials*. 2010;**20**(16):2550-2564
- [73] Roy PK, Ujjain SK, Dattatreya S, Kumar S, Pant R, Khare KJAPA. Mechanically tunable single-component soft polydimethylsiloxane (PDMS)-based robust and sticky superhydrophobic surfaces. *Applied Physics A: Materials Science & Processing*. 2019;**125**(8):535
- [74] Wang H, Zhang Z, Wang Z, Liang Y, Cui Z, Zhao J, et al. Multistimuli-responsive microstructured superamphiphobic surfaces with large-range, reversible switchable wettability for oil. *ACS Applied Materials & Interfaces*. 2019;**11**(31):28478-28486
- [75] Li Z, Liu Y, Lei M, Su A, Sridhar S, Li Y, et al. Stimuli-responsive gel impregnated surface with switchable lipophilic/oleophobic properties. *Soft Matter*. 2020;**16**(6):1636-1641
- [76] Bai D, Habersberger BM, Jennings GK. pH-responsive copolymer films by surface-catalyzed growth. *Journal of the American Chemical Society*. 2005;**127**(47):16486-16493
- [77] Xu C, Wayland BB, Fryd M, Winey KI, Composto RJ. pH-responsive nanostructures assembled from amphiphilic block copolymers. *Macromolecules*. 2006;**39**(18):6063-6070
- [78] Li J, Chen X, Chang Y-C. Preparation of end-grafted polymer brushes by nitroxide-mediated free radical polymerization of vaporized vinyl monomers. *Langmuir*. 2005;**21**(21):9562-9567
- [79] Uhlmann P, Ionov L, Houbenov N, Nitschke M, Grundke K, Motornov M, et al. Surface functionalization by smart coatings: Stimuli-responsive binary polymer brushes. *Progress in Organic Coating*. 2006;**55**(2):168-174
- [80] Lu Y, Sarshar MA, Du K, Chou T, Choi C-H, Sukhishvili SA. Large-amplitude, reversible, pH-triggered wetting transitions enabled by layer-by-layer films. *ACS Applied Materials & Interfaces*. 2013;**5**(23):12617-12623
- [81] Minko S, Müller M, Motornov M, Nitschke M, Grundke K, Stamm M. Two-level structured self-adaptive surfaces with reversibly tunable properties. *Journal of*

the American Chemical Society.  
2003;**125**(13):3896-3900

[82] Lee CH, Kang SK, Lim JA,  
Lim HS, Cho JH. Electrospun smart  
fabrics that display pH-responsive  
tunable wettability. *Soft Matter*.  
2012;**8**(40):10238-10240

[83] Wang F, Pi J, Li J-Y, Song F, Feng R,  
Wang X-L, et al. Highly-efficient  
separation of oil and water enabled  
by a silica nanoparticle coating  
with pH-triggered tunable surface  
wettability. *Journal of Colloid and  
Interface Science*. 2019;**557**:65-75

[84] Cheng Z, Lai H, Zhang N,  
Sun K, Jiang L. Magnetically induced  
reversible transition between Cassie and  
Wenzel states of superparamagnetic  
microdroplets on highly hydrophobic  
silicon surface. *Journal of Physical  
Chemistry C*. 2012;**116**(35):18796-18802

[85] Grigoryev A, Tokarev I, Kornev KG,  
Luzinov I, Minko S. Superomniphobic  
magnetic microtextures with  
remote wetting control. *Journal of  
the American Chemical Society*.  
2012;**134**(31):12916-12919

[86] Motornov M, Minko S, Eichhorn  
K-J, Nitschke M, Simon F, Stamm M.  
Reversible tuning of wetting behavior  
of polymer surface with responsive  
polymer brushes. *Langmuir*.  
2003;**19**(19):8077-8085

[87] Liu Y, Mu L, Liu B, Kong J.  
Controlled switchable surface.  
*Chemistry–A European Journal*.  
2005;**11**(9):2622-2631

[88] Wang X, Qing G, Jiang L, Fuchs H,  
Sun T. Smart surface of water-induced  
superhydrophobicity. *Chemical  
Communications*. 2009;**19**:2658-2660